

# *Caenorhabditis elegans* HUS-1 Is a DNA Damage Checkpoint Protein Required for Genome Stability and EGL-1-Mediated Apoptosis

E. Randal Hofmann,<sup>1,6,8</sup> Stuart Milstein,<sup>1,2,3,8</sup>

Simon J. Boulton,<sup>3,4</sup> Mianjia Ye,<sup>1</sup>

Jen J. Hofmann,<sup>1,6</sup> Lilli Stergiou,<sup>6</sup>

Anton Gartner,<sup>5</sup> Marc Vidal,<sup>3</sup>

and Michael O. Hengartner<sup>1,6,7</sup>

<sup>1</sup>Cold Spring Harbor Laboratory

1 Bungtown Road

Cold Spring Harbor, New York 11724

<sup>2</sup>Graduate Program in Genetics and Department of  
Molecular Genetics and Microbiology

The State University of New York at Stony Brook

Stony Brook, New York 11794

<sup>3</sup>Dana-Farber Cancer Institute

Department of Genetics

Harvard Medical School

Boston, Massachusetts 02115

<sup>4</sup>Cancer Research UK

Clare Hall

Clare Hall Laboratories

South Mimms

Hertfordshire EN6 3LD

United Kingdom

<sup>5</sup>Max-Planck-Institute for Biochemistry

Department of Cell Biology

Am Klopferspitz 18a

Martinsried 82152

Germany

<sup>6</sup>University of Zürich

Institute for Molecular Biology

Winterthurerstrasse 190

8057 Zürich

Switzerland

## Summary

**Background:** The inability to efficiently repair DNA damage or remove cells with severely damaged genomes has been linked to several human cancers. Studies in yeasts and mammals have identified several genes that are required for proper activation of cell cycle checkpoints following various types of DNA damage. However, in metazoans, DNA damage can induce apoptosis as well. How DNA damage activates the apoptotic machinery is not fully understood.

**Results:** We demonstrate here that the *Caenorhabditis elegans* gene *hus-1* is required for DNA damage-induced cell cycle arrest and apoptosis. Following DNA damage, HUS-1 relocalizes and forms distinct foci that overlap with chromatin. Relocalization does not require the novel checkpoint protein RAD-5; rather, relocalization appears more frequently in *rad-5* mutants, suggesting that RAD-5 plays a role in repair. HUS-1 is required for genome stability, as demonstrated by increased frequency of spontaneous mutations, chromosome non-disjunction, and telomere shortening. Finally, we show

that DNA damage increases expression of the proapoptotic gene *egl-1*, a response that requires *hus-1* and the *p53* homolog *cep-1*.

**Conclusions:** Our findings suggest that the RAD-5 checkpoint protein is not required for HUS-1 to relocalize following DNA damage. Furthermore, our studies reveal a new function of HUS-1 in the prevention of telomere shortening and mortalization of germ cells. DNA damage-induced germ cell death is abrogated in *hus-1* mutants, in part, due to the inability of these mutants to activate *egl-1* transcription in a *cep-1/p53*-dependent manner. Thus, HUS-1 is required for *p53*-dependent activation of a BH3 domain protein in *C. elegans*.

## Introduction

Tumorigenesis is characterized by the accumulation of genetic mutations, rearrangements, amplifications, and deletions — any of which can drive the progressive transformation of normal cells into highly malignant derivatives [1]. Cancer avoidance therefore requires precise and efficient means to maintain the integrity of the genome. Damage to DNA triggers checkpoint controls that result in cell cycle arrest and repair of the lesion. In metazoans, DNA damage often results in the programmed demise of the cell, possibly due to extensive damage that is not rectifiable [2]. Alternatively, it may be prudent for the organism to eliminate dangerous cells in tissues that have an extensive proliferative capacity, even when damage has been minimal [3, 4]. Loss of communication between the DNA lesion and the apoptotic program, which allows the persistence of cells with damaged and/or unstable genomes, can lead to tumorigenesis.

Our understanding of the genetics of the DNA damage checkpoint pathway has been heavily dependent on studies done in the yeasts *Saccharomyces cerevisiae* and *Schizosaccharomyces pombe* [5]. The DNA damage checkpoint in *S. pombe* includes six “rad” genes: *rad1*<sup>+</sup>, *rad3*<sup>+</sup>, *rad9*<sup>+</sup>, *rad17*<sup>+</sup>, *rad26*<sup>+</sup>, and *hus1*<sup>+</sup>. DNA damage activates Rad3, a phosphatidylinositol kinase family member that is structurally and functionally related to human ATM and ATR [6]. Rad3 is required for phosphorylation of Hus1, Rad26, Chk1, and Cds1. Phosphorylation of the kinases Chk1 and Cds1 transduces DNA damage and replication checkpoint signals to the cell cycle machinery [5]. Despite our exceptional understanding of checkpoint arrest and repair, yeast lack an apoptotic program; thus, our understanding of how a cell decides to repair or die is lagging.

The genetics of apoptosis has been extensively studied in the nematode *Caenorhabditis elegans* [7]. Although the majority of this work has focused on developmental aspects of somatic apoptosis, recent research has also focused on the germline [8]. Unlike the invariable pattern of somatic cell deaths during development, germline apoptosis is not determined by lineage and can

<sup>7</sup> Correspondence: michael.hengartner@molbio.unizh.ch

<sup>8</sup> These authors contributed equally to this work.

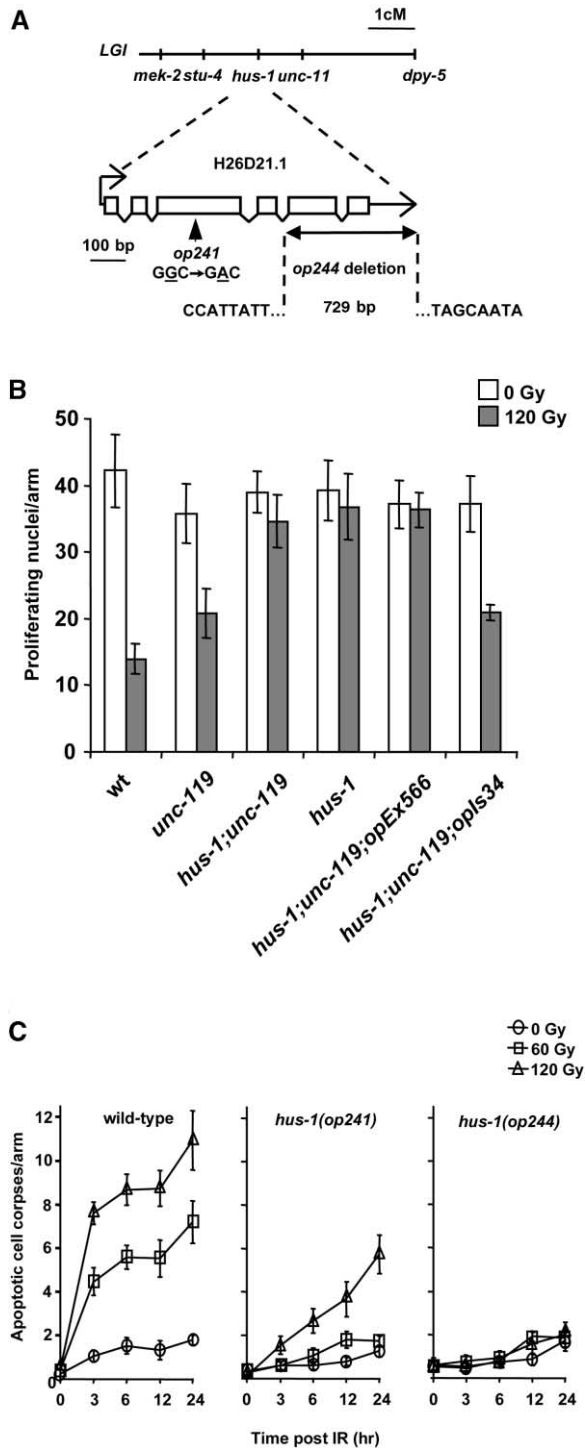


Figure 1. Identification of *hus-1* Mutants

(A) Genetic map and genomic structure of the *hus-1* gene. Boxes represent coding sequence. The position and nature of the *hus-1* mutations are indicated.

(B) Quantification of cell proliferation arrest in wild-type, *hus-1(op241)*, and *hus-1(op241);unc-119(ed3)* strains with integrated *opIs34* and nonintegrated (*opEx566*) transgenic constructs. The number of cells in the proliferating region of the germline was viewed by DIC and scored 50  $\mu$ m from the distal end of the gonad 12 hr following irradiation, as described in Supplementary Experimental Procedures. Each bar represents five worms  $\pm$  SD.

be regulated by multiple pathways. We have previously demonstrated that *C. elegans* is an excellent genetic tool that can be used to understand DNA damage-induced cell cycle arrest and apoptosis [9, 10]. DNA damage-mediated apoptosis is dependent on *ced-3* and *ced-4* and is negatively regulated by *ced-9*. The positive death regulator, *egl-1*, is partially required, but it is not essential for radiation-induced apoptosis. Recently, three *C. elegans* checkpoint mutants, *op241*, *rad-5(mn159)*, and *mrt-2(e2663)*, have been identified that block DNA damage-induced apoptosis and cell cycle arrest [9, 11]. It is unclear how these checkpoint genes regulate the apoptotic machinery. One possibility is by means of a p53 homolog, *cep-1*, which is required for DNA damage-induced germ cell death but not cell cycle arrest [12, 13].

Here we show that *op241* is a hypomorphic allele in the *C. elegans* homolog of the *S. pombe* *hus1*<sup>+</sup> checkpoint gene. *hus-1* mutants fail to induce apoptosis and proliferation arrest following DNA damage and show increased sensitivity to DNA damage-induced lethality. Using a newly identified candidate null allele, we show that *hus-1* function is also required for telomere length maintenance. HUS-1 is a nuclear protein that is expressed in early embryos and the adult germlines and relocalizes to putative sites of DNA damage. Finally, we demonstrate that DNA damage induces the proapoptotic gene *egl-1*. This is dependent on *hus-1* and the p53 homolog, *cep-1*.

## Results

### Identification of Mutations in *C. elegans* *hus-1*

We have previously described mutants defective in cell cycle arrest and apoptosis induced by DNA damage [9, 10]. Included in this group was the mutation *op241*, originally identified in a strain containing the *him-7(e1480)* mutation and later named *dam-1(op241)* (DNA damage response) [9, 10]. We mapped *op241* to a 2.1-cM interval, between *stu-4* and *unc-11*, on the left side of chromosome I (Figure 1A). An in silico search for candidate genes in this interval identified *H26D21.1*, a homolog of the *S. pombe* gene *hus1*<sup>+</sup>. Sequence analysis of *H26D21.1* from *op241* revealed a G to A transition at base pair +296, resulting in a G to D substitution at amino acid 99. Because of the high sequence conservation between *H26D21.1* and *hus-1* homologs from other species, we renamed this gene *hus-1*.

In an independent reverse genetic screen for deletions in *C. elegans* homologs of known checkpoint genes, we recovered a single *hus-1* allele, *op244*. The *op244* allele is a 729-bp deletion that removes the last two exons and most of the 3' untranslated region of *hus-1* (bp 4725–5453 on cosmid H26D21) (Figure 1A). *hus-1(op244)* mutants from homozygous parents show an

(C) Comparison of the germline apoptotic response to irradiation between wild-type and *hus-1* mutants. Corpses were scored in the distal arm of the gonad of adult animals following indicated doses of irradiation. *hus-1* deletion mutants are completely defective for DNA damage-induced apoptosis; however, physiological germ cell death is present.

Table 1. *hus-1* Deletion Mutants Display Chromosome Nondisjunction and Embryonic Lethality

Genotype	F3		F3		F6	
	Males (%)	Brood Size	Survival (%)	Brood Size	Survival (%)	
Wild-type; n = 15	0.0 ± 0.0	257.4 ± 13.5	99.5 ± 2.6	239.1 ± 21.3	99.2 ± 4.3	
<i>hus-1(op241)</i> ; n = 10	0.2 ± 0.2	303.6 ± 25.9	96.9 ± 2.3	334.7 ± 24.4	96.2 ± 3.6	
<i>hus-1(op244)</i> ; n = 15	5.7 ± 10.3	222.5 ± 90.0	78.5 ± 15.7	60.1 ± 41.8	50.0 ± 17.6	

incompletely penetrant maternal effect embryonic lethality (Table 1). Complementation tests confirmed that *op241* and *op244* are allelic (see the Experimental Procedures). An extrachromosomal array (*opEx566*) of a full-length translational fusion of HUS-1::GFP under the control of the *hus-1* promoter, which does not express in the germline, fails to rescue both cell cycle arrest and DNA damage-induced apoptosis in *op241* (Figure 1B). However, a germline-expressing transgene, *opls34*, of the same construct fully rescues the DNA damage cell cycle arrest and partially rescues the apoptotic defect of *op241* (4.2-fold induction of apoptotic cells in *op241;unc-119;opls34* animals compared to 1.3-fold induction in *op241;unc-119;opEx566* and 8.6-fold induction in wild-type) (Figure 1B).

#### DNA Damage Responses Are Defective in *hus-1* Mutants

Ionizing radiation induces several responses in *C. elegans*, including germ cell apoptosis, cell cycle arrest, and embryonic lethality [9]. We have previously shown that *op241* is defective for DNA damage-induced germ cell death and cell cycle arrest [9]. We found that the *op244* allele had more severe defects in both of these responses (Figures 1C, S1A, and S1B; Figure S1 is contained in the Supplementary Material available with this article online). In addition, *op244* is more sensitive to the embryonic lethal effects of ionizing radiation (Figure S1C).

#### *hus-1(op241)* Disrupts a Checkpoint Protein Interaction

The G99D mutation in *op241* affects a residue that, while poorly conserved at the primary sequence level, borders a helix that has been proposed to interact with *S. pombe* and human Rad9 proteins (Figure 2A) [14]. Although *C. elegans* HUS-1 does not interact with HPR-9, the *C. elegans* homolog of Rad9, on its own in the two-hybrid system [15], in vivo interaction in worms is likely (see below). To analyze the molecular nature of the *hus-1(op241)* defect, we tested the mutant form of the protein for its ability to interact with four proteins (MRT-2, PDI-2, K21H4.1, and F56D12.5) that interact with HUS-1 in the yeast two-hybrid system [15]. HUS-1(+) interacted with these four proteins with varying degrees (Figure 2B). In contrast, HUS-1(G99D) is defective for its ability to interact with the conserved checkpoint protein MRT-2, the *C. elegans* homolog of *S. pombe* Rad1, and with PDI-2, a protein disulfide isomerase homolog, in the yeast-two hybrid system (Figure 2B).

Furthermore, HUS-1(G99D) failed to interact with MRT-2 in GST pull-down experiments from transfected cells (Figure 2C). However, HUS-1(+) and HUS-1(G99D)

interacted comparably with F56D12.5 and K12H4.1 (Figure 2A). These findings suggest that the *op241* mutation does not completely abolish the structural integrity of the mutant protein but specifically compromises a protein interaction domain that is important for association with MRT-2 and PDI-2. Our findings suggest that an inability to form a HUS-1/MRT-2 complex in vivo compromises the integrity of the DNA damage checkpoint in *op241*, thus providing a molecular explanation for this mutation.

#### HUS-1 Is a Nuclear Protein that Requires the Checkpoint Proteins MRT-2 and HPR-9, but Not RAD-5, for Proper Localization

*S. pombe* Hus1 p has been shown to be a nuclear protein [16]. Microscopic analysis of *opls34[hus-1::gfp]* animals revealed HUS-1::GFP localization in the nuclei of proliferating germ cells, meiotic germ cells, mature oocytes, and embryos (Figure 3A). We also observed nuclear GFP expression in a subset of somatic cells, particularly proliferating cells, in larvae (data not shown). Rad1, Rad9, and Hus1 form a heterotrimer complex that structurally resembles the proliferating cell nuclear antigen (PCNA) trimer [14, 17]. Rad17 is believed to load this complex onto DNA at or near sites of DNA damage [18]. To determine the role of these interactions in *C. elegans*, we analyzed HUS-1::GFP expression in a *mrt-2(e2663)* background. Surprisingly, the expression of HUS-1::GFP in the germline was greatly reduced and was excluded from the nucleus (Figure 3A). Crossing these worms back to wild-type worms restored proper localization of HUS-1::GFP to the nucleus (data not shown). This reduction of expression is likely due to degradation, possibly as a result of improper localization, rather than transcriptional regulation, as GFP under the control of the *hus-1* promoter (*opls29(pRH04)*) was not affected by loss of MRT-2 (data not shown).

We also analyzed the expression of HUS-1::GFP in a *rad-5(mn159)* background. RAD-5 is homologous to *S. cerevisiae* Tel2p and is required for germ cell replication and DNA damage checkpoints [9, 11]. HUS-1::GFP localization was not different in *rad-5(mn159)* than in the parental strain (Figure 3A), and this finding is consistent with evidence that *rad-5* acts independently of *hus-1* and *mrt-2* [11]. Interestingly, HUS-1::GFP levels were significantly lower in *rad-5(mn159)* mutants compared to the parental strain.

MRT-2 interacts with HPR-9 in a two-hybrid assay, suggesting that the Rad1/Rad9/Hus1 complex is conserved in *C. elegans* [15]. Inhibition of *hpr-9* expression via RNAi was sufficient to disrupt HUS-1::GFP localization and expression similarly to a *mrt-2* RNAi-positive control, indicating that HPR-9 is also required for HUS-1

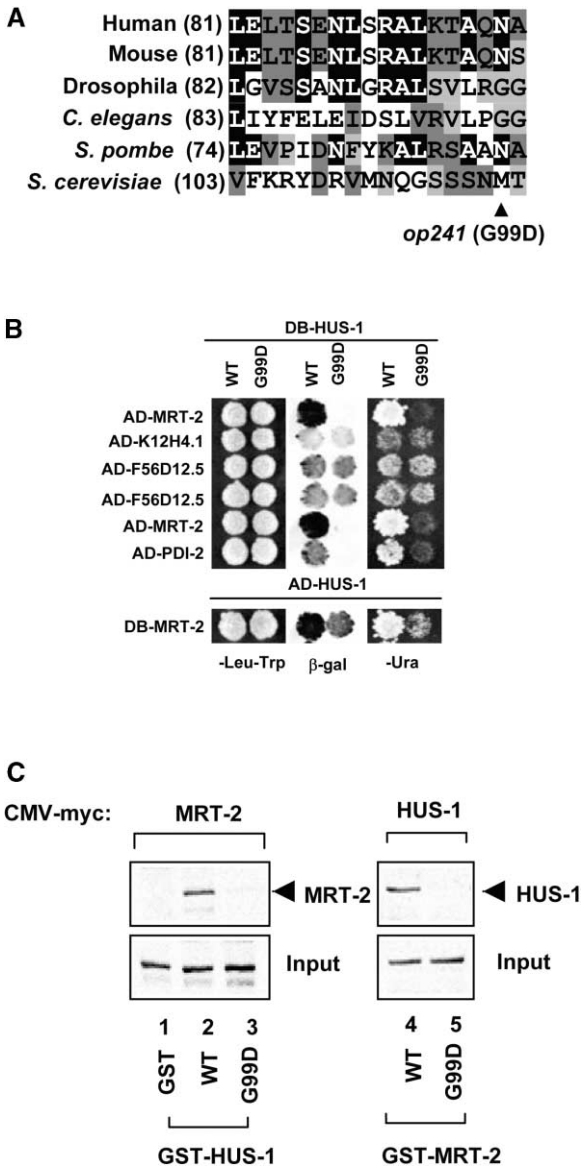


Figure 2. HUS-1(G99D) Is Defective for MRT-2 and PDI-2 Binding (A) Using the Blosum62mt2 matrix (Align-X), the alignment of the putative helical Rad9 interacting region of Hus1 from human, mouse, fly, worm, and fission yeast and Mec3 from budding yeast was determined. The affected residue in *op241* is indicated by an arrowhead. See text for details.

(B) The yeast two-hybrid system was used to test for protein interactions with wild-type (WT) and mutant (G99D) HUS-1-GAL4 DNA binding domain (DB) fusions by scoring for LacZ expression and growth on -Ura plates (no selection: -Leu -Trp). HUS-1(WT) interacts with GAL4 activation (AD) fusions of MRT-2, K12H4.1, F56D12.5, and PDI-2. HUS-1(G99D) does not interact with MRT-2 and PDI-2, but it still interacts with K12H4.1 and F56D12.5.

(C) In vitro interaction of HUS-1 and MRT-2. GST-HUS-1(WT), but not GST-HUS-1(G99D) or GST alone, interacts with Myc-epitope-tagged MRT-2 (lanes 1-3). GST-MRT-2 is able to interact with wild-type (WT) but not mutant Myc-epitope-tagged HUS-1(G99D) (lanes 4 and 5).

localization and stabilization (Figure 3B). In contrast, *hpr-17(RNAi)*- and *ced-3(RNAi)*-treated worms showed normal HUS-1::GFP localization (Figure 3B). HUS-

1::GFP nuclear localization is independent of the other HUS-1-interacting proteins that we tested (PDI-2, K21H4.1, and F56D12.5; data not shown).

### HUS-1::GFP Relocalizes to Distinct Foci that Colocalize with Chromatin following DNA Damage

In order to determine the subcellular localization of HUS-1 following DNA damage, we analyzed HUS-1::GFP localization in germ cells before and after exposure to ionizing radiation. HUS-1::GFP was diffuse in proliferating germ nuclei and weakly chromatin localized in pachytene cells under normal conditions. However, following exposure to ionizing radiation, HUS-1::GFP concentrates at distinct nuclear foci in all stages of germ cell development (Figures 4A, 4C, and 4D). The presence of these foci could be observed as early as 3 hr following exposure to ionizing radiation. These foci overlap with chromatin, as demonstrated by counterstaining with DAPI (Figures 4C and 4D).

Genetic evidence of increased DNA damage sensitivity in *hus-1(op241);rad-5(mn159)* and *rad-5(mn159) mrt-2(e2663)* double mutants suggest that *rad-5* functions in a parallel pathway to *hus-1* and *mrt-2* [11]. In order to determine if relocalization of HUS-1::GFP was dependent on *rad-5*, we irradiated worms containing the *hus-1::gfp* transgene in a *rad-5(mn159)* background. We found that rather than being blocked, HUS-1::GFP relocalization was enhanced in the absence of *rad-5* function. The number of foci were present in greater numbers in the absence of RAD-5 prior to and after exposure to ionizing radiation (Figure 4B). Further, we found that, while HUS-1::GFP foci numbers decreased in *rad-5(+)* controls after 20 hr, the number of foci did not change in *rad-5* mutants (Figure 4B).

Double-strand breaks also occur under normal conditions during meiotic prophase from initiation events during recombination. These double-strand breaks fail to "heal" in several yeast mutants, resulting in pachytene cell cycle arrest. RNAi of the RecA-strand exchange family member, *rad-51*, similarly blocks recombination in *C. elegans* germ cells and results in increased germ cell apoptosis [9, 19]. Under normal conditions, a limited number of HUS-1::GFP foci can occasionally be observed in the pachytene region of the germline (Figure 4D). In contrast, *rad-51(RNAi)* worms showed a dramatic increase in HUS-1::GFP foci (Figure 4D).

### The *hus-1* Deletion Mutant Exhibits Genome Instability

Several lines of evidence suggest that loss of *hus-1* function leads to genomic instability. First, *hus-1* mutants show high levels of chromosomal nondisjunction, as evidenced by the high proportion of males (the result of X chromosome nondisjunction) in the self-progeny of *op244* mutants. Whereas nondisjunction of the X chromosomes produces less than 0.2% male progeny in the wild-type [20], early *op244* generations produce about 6% males (Table 1). Second, as has been observed for other mutants defective in genome stability, *hus-1* mutants show abnormal levels of embryonic lethality [21]: early generations of *op244* mutants produce about

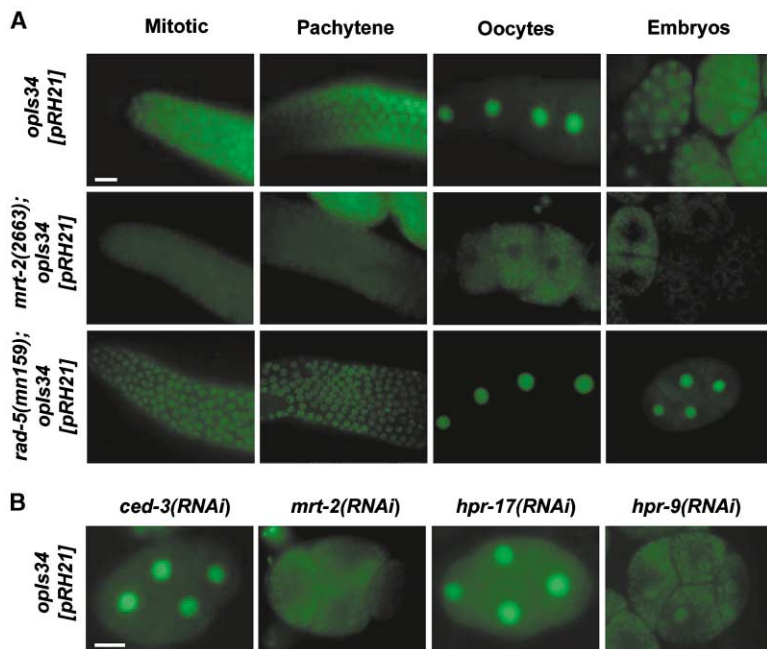


**Figure 3. HUS-1 Nuclear Localization Requires MRT-2 and HPR-9**

(A) Fluorescent microscopy of integrated transgenic strains expressing fusion constructs in gonads and embryos of wild-type, *mrt-2(e2663)*, and *rad-5(mn159)* mutant backgrounds. The genotype and construct used are indicated, and expression is shown in the indicated stage of oogenesis and early embryos. pRH21 is a full-length translational fusion containing 2252 bp of genomic sequence 5' to the stop codon.

(B) Fluorescent microscopy of 4-cell-stage embryos from F2-integrated transgenic worms fed dsRNA produced from indicated genes as described in the Experimental Procedures. For confirmation of *ced-3(RNAi)* and *hpr-17(RNAi)*, germ cell death and hypersensitivity to radiation-induced embryonic lethality, respectively, were scored. The scale bars represent 10  $\mu$ m.

78% healthy progeny that survive to adulthood (the level of larval lethality was minimal) (Table 1). Embryonic survival is even lower in later generations. Embryonic survival of *op241* mutants was not significantly different from wild-type worms. Nondisjunction of autosomes could well explain most or all of the embryonic lethality seen in *op244* mutants, although other defects, such as failure to repair endogenous damage, cannot be excluded. Indeed, spontaneous mutations are more frequent, as measured by an *unc-93* reversion assay (see below).

Mutations in the checkpoint gene *mrt-2* result not only in a failure to induce apoptosis in response to DNA damage [9], but also in progressive telomere loss, eventually leading to end-to-end chromosome fusion and aneuploidy [22]. As a consequence of these defects, the brood sizes of *mrt-2* mutants decrease over generations until the animals become sterile – the Mrt (mortal germline) phenotype from which the gene derived its name. While early generations of freshly outcrossed *op244* mutants have brood sizes similar to wild-type worms, later generations showed dramatically lower fertility (Table 1) and became sterile after about 15 generations (producing very few embryos, none of which hatch). We did not see a Mrt phenotype in *op241* mutants kept at 20°C (Table 1). However, when grown at 25°C, *op241* mutants also became sterile after approximately 15 generations, suggesting that *op241* might be a temperature-sensitive allele.

To test whether the Mrt phenotype of *hus-1* mutants was due to telomere loss, we probed Southern blots of genomic DNA from multiple generations of *op244* and *op241* strains. In *op244* mutants grown at 20°C, we saw a progressive loss of telomere sequence in late generations of worms (Figure 5A). As reported before, the ends of telomeres do not decrease in *op241* mutants grown at 20°C [11]; however, worms grown at 25°C did display telomere shortening (data not shown). In wild-type

worms, six chromosomal bivalents can be observed by DAPI staining of oocytes in diakinesis. In contrast, late generations of *op244* mutants often contained fewer than six bivalents. In *op244* generations no longer producing viable progeny, only 3–4 bivalents could be seen (Figure 5B); consistent with the idea that loss of telomeres led to chromosome fusions. Correspondingly, the incidence of males increases dramatically after several generations and gives rise eventually to dominant Him (high incidence of males) strains (data not shown).

One function of checkpoint genes is to prevent cells with a damaged genome from progressing through the cell cycle without correcting the DNA lesion. Mutations in genes that repair these lesions or regulate the checkpoints that prevent cell cycle progression have been shown to display higher spontaneous mutation frequencies [23, 24]. Since *hus-1* has a checkpoint function, we used the well-characterized *unc-93* reversion assay to look at spontaneous mutation frequencies in *hus-1* worms [25]. We found the spontaneous suppression frequency of *unc-93(e1500)* worms in our assay to be  $1 \times 10^{-6}$  (Figure 5C). In two independent *hus-1(op244);unc-93(e1500)* strains, we found the mutation frequency to be 10- to 20-fold higher than in the control strain (Figure 5C). Consistent with this, the appearance of spontaneous mutations has also been observed during strain maintenance (data not shown).

#### Ionizing Radiation Induces *egl-1* Transcript Upregulation in a *hus-1*- and *cep-1*-Dependent Manner

In order to determine whether *hus-1* is transcriptionally regulated following DNA damage, we isolated mRNA from adult wild-type and *hus-1(op244)*-irradiated worms and probed Northern blots with *hus-1* cDNA. A single transcript of the expected size was seen in wild-type; however, the transcript was truncated and levels were dramatically reduced in the *hus-1(op244)* deletion mu-

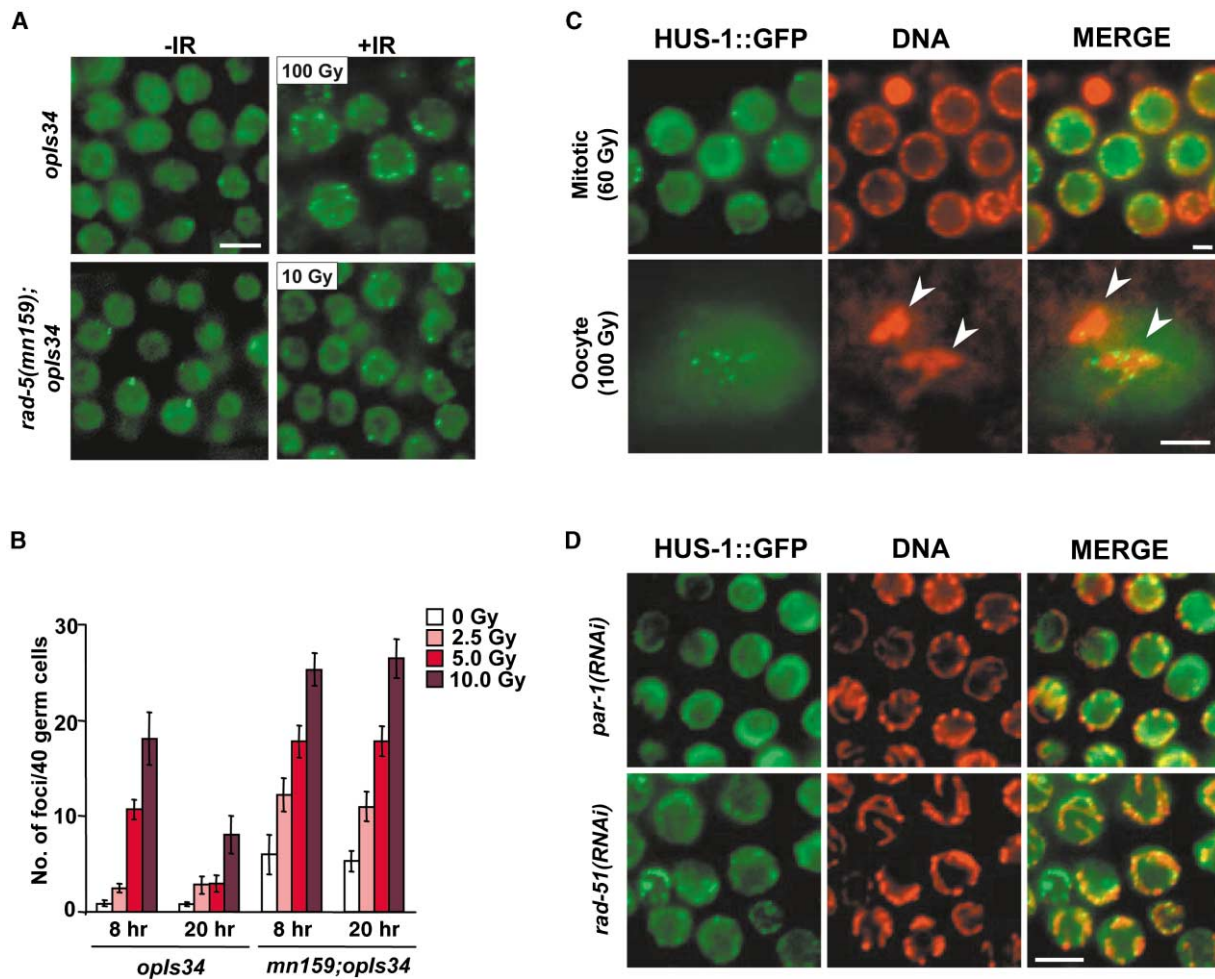


Figure 4. Subcellular Relocalization of HUS-1::GFP following DNA Damage

(A) Fluorescent microscopy of proliferating germ cells expressing HUS-1::GFP (*opls34*). Irradiated worms (*opls34* = 100 Gy; *rad-5(mn159);opls34* = 10 Gy) were viewed 8 hr following irradiation. HUS-1::GFP is diffuse in controls. Relocalized HUS-1::GFP is seen as bright foci. The scale bar represents 5  $\mu$ m.

(B) Quantification of HUS-1::GFP foci in wild-type and *rad-5(mn159)* backgrounds. Foci were scored in 40 proliferating germ cells in a single Z stack following mild doses of X-rays at indicated times. Each bar represents ten worms  $\pm$  SEM.

(C) Colocalization of HUS-1::GFP with chromatin following exposure to ionizing radiation. The top panel shows proliferating germ cells. The bottom panel shows a single oocyte nucleus in diakinesis. Arrowheads point to two DAPI-stained bivalents from an oocyte in diakinesis. The scale bar represents 2  $\mu$ m.

(D) Fluorescent microscopy of meiotic germ cells from worms fed dsRNA from *rad-51* and a *par-1* control. As in (C), HUS-1::GFP foci overlap with chromatin stained with Hoechst 33342 dye. The scale bar represents 5  $\mu$ m.

tant. Levels of *hus-1* mRNA did not change significantly 60 and 180 min after exposure to IR (Figure 6A).

In *C. elegans*, the BH3 domain protein, EGL-1, activates the apoptotic machinery. Furthermore, *egl-1* is transcriptionally regulated in order to activate apoptosis during somatic development [26]. We subsequently hybridized the same blot to an *egl-1* probe. We found that, in wild-type young adults, *egl-1* is induced by 60 min and increases by 180 min after irradiation (Figures 6A and 6B). Induction is significantly lower in *glp-4(bn2)* (a temperature-sensitive mutant that lacks a germline at the restrictive temperature) animals, suggesting that *egl-1* induction is largely restricted to the germline (Figure 6B). Consistent with this hypothesis, we found germline induction of an *egl-1::gfp* transcriptional reporter

construct following exposure to ionizing radiation (Figure 6C). Importantly, *egl-1* levels did not increase in the *hus-1(op244)* deletion worms after irradiation (Figures 6A and 6B). These results are consistent with the hypothesis that *hus-1*-dependent induction of *egl-1* transcription is an important element of the apoptotic DNA damage response in *C. elegans* and that it promotes the increased germ cell apoptosis observed following genotoxic stress.

Recent work showed that the *cep-1* gene, which encodes a *C. elegans* homolog of p53, is required for DNA damage-induced germ cell apoptosis [12, 13]. In order to determine if *cep-1* is also required for *egl-1* induction, we analyzed *egl-1* expression by using real-time quantitative RT-PCR (Q-RT-PCR) before and after exposure to



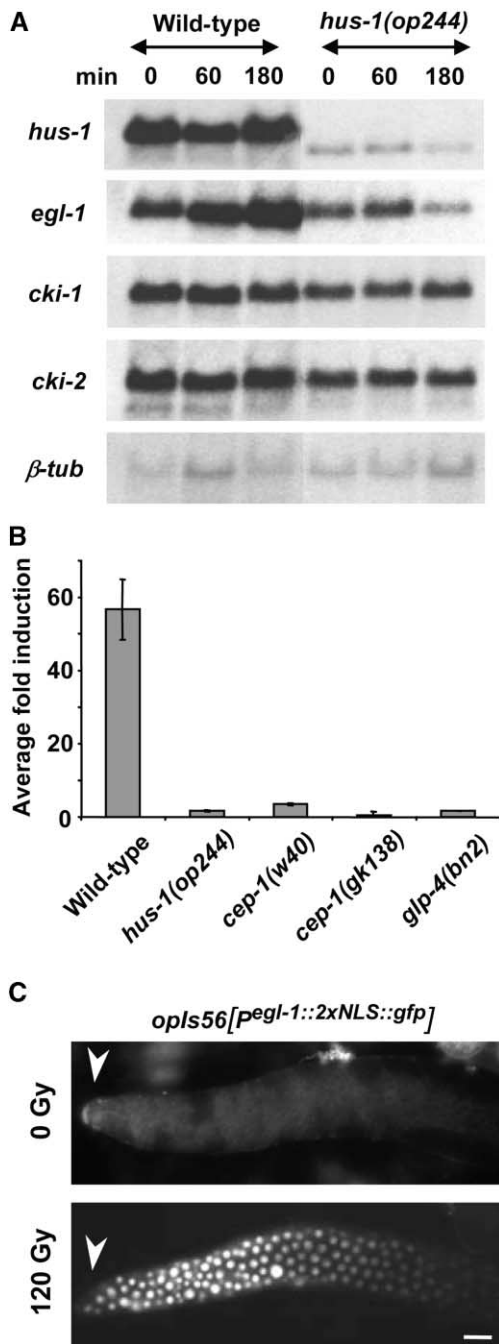


Figure 6. *egl-1* Is Transcriptionally Induced by Irradiation in a *hus-1*- and *cep-1*-Dependent Manner

(A) Northern blots were performed with 2  $\mu$ g polyA-enriched RNA isolated from wild-type and *hus-1(op244)* mutant young adult worms at indicated times after exposure to 120 Gy  $\gamma$ -irradiation. The same blot was reprobed with a PCR-generated probe from the indicated gene on the left.

(B) Average fold induction of *egl-1* gene expression in wild-type, *hus-1(op244)*, *cep-1(w40)*, *cep-1(gk138)*, and *glp-4(bn2)* mutants after 100 Gy X-ray irradiation as determined by real-time quantitative RT-PCR. *glp-4(bn2)* worms were grown at the nonpermissive temperature, and 90–100 worms were selected that lacked a germline. Each bar represents the average  $\pm$  SD.

(C) Induction of *egl-1::gfp* expression in the germline. A construct containing 2.7 kb of genomic sequence 5' to the translation start

tenance of genome stability. Deletion mutants show a high frequency of meiotic nondisjunction and/or chromosome loss, resulting in increased male progeny, due to loss of the X chromosome, and high levels of embryonic lethality. Chromosome abnormalities have also been reported in mouse *Hus1*<sup>-/-</sup> cells [30]. One possible cause for the increase in genome instability is the inability to recognize or repair various forms of DNA damage. Indeed, we found that *hus-1* mutants have a mutator phenotype.

Our results also demonstrate that, unlike in yeast, HUS-1 is required for the prevention of telomere shortening during replication of the genome [31]. *hus-1* deletion worms show a progressive shortening of telomeres, which is associated with a progressive reduction in brood size, reaching complete sterility by the 15<sup>th</sup> generation. In late-generation worms, outcrossing reveals a dominant Him phenotype that is consistent with end-to-end fusions of the X chromosome with autosomes, due to loss of telomeric ends [22]. Fusions are also apparent in oocytes of late-generation worms in which only three or four bivalents, rather than the typical six, can be detected in diakinesis. A similar mortal germline phenotype and chromosome fusions associated with telomere loss have previously been reported for a mutant in the HUS-1-interacting protein MRT-2, and this finding suggests that the same MRT-2/HUS-1 complex that acts in checkpoint control might also control telomere length. It is not known what role HUS-1 has in telomere maintenance in vertebrates.

Studies of DNA damage responses in *C. elegans* have revealed intriguing differences from responses in mammals. DNA damage induces both a G1/S and G2/M arrest in mammalian cells. These cell cycle arrest checkpoints are mediated, in part, by the cyclin kinase inhibitor p21 in a p53-dependent manner [29]. However, we did not see an increase of mRNA levels of two candidate cyclin kinase inhibitors, *cki-1* and *cki-2*, at the times examined. It remains possible that one or both of these CIP homologs is induced at later time points or is posttranscriptionally regulated. Unlike in mammals, but similarly to *Drosophila* [32], loss of CEP-1 (p53) function in *C. elegans* does not result in a cell cycle arrest defect in response to DNA damage [12, 13], suggesting that induction of apoptosis might have been the original function of p53 family members during evolution. Mutants of the homologs of yeast Cdc2 and Cdc25 have been shown to disrupt normal cell cycle in the germline of *C. elegans*; thus, as in yeast, these are possible candidates for downstream effectors of HUS-1-mediated checkpoints [33, 34].

In mammalian cells, DNA damage induces the tran-

site of *egl-1* fused to GFP equipped with two nuclear localization signals. Worms were synchronized and irradiated as L4 animals. GFP expression was analyzed in dissected gonads 30 hr following irradiation. Expression was seen in both proliferating and late-pachytene germ cells in most (12/16) irradiated animals. Background expression could be seen in the late-pachytene germ cells in few (2/23) nonirradiated controls, but not (0/23) in the proliferating germ cells. The arrowhead indicates the distal end of the gonad. The scale bar represents 10  $\mu$ m.

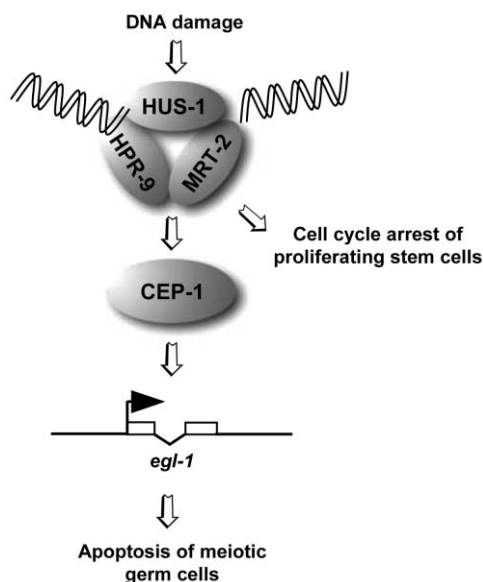


Figure 7. Model: A Pathway for DNA Damage-Induced Apoptosis and Cell Cycle Arrest in *C. elegans*

DNA damage recruitment of the HUS-1/MRT-2/HPR-9 complex to the site of the lesion, where it activates cell cycle arrest of proliferating stem cells. This complex also signals to the apoptotic machinery via CEP-1-dependent upregulation of *egl-1*.

scription of many genes, including the proapoptotic BH3 domain-containing proteins Bax, Puma, and Noxa [35–38]. Transcriptional activation of Bax is dependent on p53 in a tissue-dependent manner but is independent of Atm [39]. However, it is not known whether the genes that sense damaged DNA, such as the Rad family proteins, are required for the induction of Bax, Puma, or Noxa. We demonstrate in *C. elegans* a dramatic increase in mRNA levels for the proapoptotic protein EGL-1 following irradiation. We conclude that this induction is mostly in the germline, as *glp-4* mutants lack strong *egl-1* induction and a GFP reporter displayed high germline expression following irradiation. Induction of *egl-1* by  $\gamma$ -irradiation is dependent on *hus-1*. This provides a molecular explanation for how DNA damage induces apoptosis in germ cells of *C. elegans* and suggests a key link between a DNA damage checkpoint gene and the apoptotic machinery (Figure 7). However, as in mammals, DNA damage likely activates other proapoptotic genes since *egl-1(lf)* mutants are only partially defective in this response.

In mice, all *Hus1*<sup>−/−</sup> embryos die by 11.5 days post-coitum (dpc) [30], and this death is at least in part due to a high level of chromosome abnormalities, which result in increased apoptosis during embryogenesis. Similarly, we showed that, while worm HUS-1 is not absolutely required for embryonic survival, a significant fraction of *hus-1* embryos die during embryogenesis, likely due to genomic instability. However, we failed to detect any increase in somatic developmental cell death in *hus-1* mutants (data not shown), and these findings are consistent with our previous report that DNA damage does not induce somatic cell apoptosis [9].

In *C. elegans*, p53 function is essential for *hus-1*-medi-

ated apoptosis. In contrast, p53 status does not influence apoptosis and embryonic lethality in *Hus1*<sup>−/−</sup> mice, as the *Hus1*<sup>−/−</sup>*p53*<sup>−/−</sup> embryonic lethality is morphologically indistinguishable from that of *Hus1*<sup>−/−</sup> embryos [40]. Furthermore, induction of p53 target genes, such as Bax, is normal in *Hus1*<sup>−/−</sup> mice. However, in *C. elegans*, induction of *egl-1* requires *hus-1* and the p53 homolog, *cep-1*. Thus, unlike in mouse embryos [40], *hus-1* and *cep-1* likely act in a common pathway to activate the apoptotic machinery (Figure 7).

In contrast to *hus-1(op244)* mutants, which are highly sensitive to IR-induced double-strand breaks (DSBs), mouse *Hus1*<sup>−/−</sup> cells are highly sensitive to hydroxyurea (HU) and ultraviolet (UV) radiation, but not to ionizing radiation (IR) [30]. One explanation may be that Hus1 in mice is required primarily for the replication checkpoint (UV and HU), but not the DSB checkpoint (IR) during embryogenesis. Indeed, lack of Hus1 or low levels of IR fail to induce cell cycle arrest in mouse embryos; however, apoptosis is induced [4, 30]. However, HUS1, along with Atm and p53, may also play a primary role in responding to DSBs after cells become more differentiated [41]. In several knockouts (*Hus1*<sup>−/−</sup>, *Atm*<sup>−/−</sup>, *Brca*<sup>−/−</sup>), apoptotic cells have been shown to have constitutively higher levels of Bax. Here we demonstrate that, in *C. elegans*, loss of DNA damage sensors upstream of p53 results in loss of activation of the apoptotic machinery and results in radioresistant cells. As with the loss of p53, this may be a crucial step toward transformation into malignant tumors [42].

While the deletion mutant *hus-1(op244)* shows evidence of embryonic defects due to genomic instability and telomere loss, *hus-1(op241)* only appears to be defective in the DNA damage checkpoint response under normal laboratory growth conditions. The fact that mutations can disrupt checkpoint function without impairing essential genome maintenance functions during embryogenesis (chromosome segregation) and oogenesis (telomere maintenance) in *C. elegans* might explain how checkpoint genes essential for viability in mammals can also act as tumor suppressors. For example, even though *Chk1*<sup>+/-</sup> (in a *Wnt-1* oncogenic background) and *Atr*<sup>+/-</sup> can promote tumorigenesis, loss of heterozygosity is not seen in these tumors, because loss of either *Atr* or *Chk1* is cell lethal [43, 44]. Thus, while complete loss of DNA damage checkpoint genes can induce mitotic catastrophe, more subtle mutations may contribute to oncogenic transformation by preventing cell cycle arrest and apoptosis.

## Conclusions

*C. elegans* HUS-1 is a conserved checkpoint protein that is required for DNA damage-induced cell cycle arrest and apoptosis. Following DNA damage, HUS-1 relocates to putative sites of DSBs independently of the novel checkpoint protein RAD-5. HUS-1 is also required for genome stability and telomere maintenance. We also demonstrate that HUS-1 checkpoint, but not essential genome maintenance, functions are dispensable for embryogenesis, suggesting a possible requirement for HUS-1 in tumor suppression. DNA damage upregulates EGL-1 in a HUS-1- and CEP-1-dependent manner, pro-

viding a molecular link between DNA damage sensors and p53-mediated activation of BH3 proteins in *C. elegans*.

#### Experimental Procedures

##### Isolation of *op244*

A deletion library was constructed by using trimethylpsoralen and UV mutagenesis as previously described [45]. This library was screened for deletion mutants of *H26D21.1* via nested PCR by using the following primer sequences: first round 5'-ATGGTCTGCAGG GAAATAG-3' and 5'-ATCCGTTAACAGTGAGATACTC-3' and nested 5'-AGGCACATACAATAACGGTG-3' and 5'-ATCACGATCATGT GAAGCCG-3'. Pooled genomic DNA from 96-well plates was screened, and positive plates were screened again by rows and columns to get a single well address. Thawed worms from a positive address were screened by single worm PCR to confirm the presence of the mutation. Homozygous worms were used to prepare genomic DNA for sequence analysis of the mutated *H26D21.1* gene. *op244* mutants were backcrossed to the wild-type eight times before phenotypic analysis.

##### Spontaneous Mutation Frequencies of *op244*

Mutants of each genotype were singled (*unc-93*,  $n = 100$ ; *hus-1;unc-93* F1.1,  $n = 88$ ; *hus-1;unc-93* F1.2,  $n = 83$ ) and monitored for three generations until plates were starved. Starved animals were then transferred to new plates, and the number of plates with revertants were scored as independent reversion events (*unc-93*, 6/100; *hus-1;unc-93* F1.1, 47/88; *hus-1;unc-93* F1.2, 27/83). These events were then divided by the total number of haploid genomes screened, based on the average brood size of each genotype, to determine the reversion frequency.

##### Transgenic Worms

HUS-1::GFP lines were constructed with pRH04 and pRH21. pRH04 is a transcriptional fusion containing 1144 bp of genomic sequence upstream of the start codon. pRH21 is a translational fusion construct containing 2252 bp including upstream regulatory sequence and all coding sequence of *H26D21.1* fused in-frame to the C-terminal GFP tag. pRH21 contains GFP and *let-858* sequences from pPD117.01 (gift of A. Fire) and rescuing *unc-119* genomic sequence from pDPM016 [46]. pRH25 was made by subcloning a 2.7-kb PCR fragment of the sequence 5' to the *egl-1* start codon into pRH20, which contains a Kpn-1 and Apal (2xNLS::GFP::let-858'UTR) fragment from pPD135.83 (gift of A. Fire) and the *unc-119(+)* rescuing sequence. Constructs were bombarded into *unc-119(ed3)* worms as previously described [46]. Integration of each construct was determined by loss of visible *Unc-119* offspring. At least three integrated lines were generated for each construct. Gonads were dissected and were stained with Hoechst 33342 (0.5  $\mu$ g/ml) or were fixed with 4% paraformaldehyde followed by cold methanol and stained with DAPI (0.2  $\mu$ g/ml). Images were captured with an ORCA-ER digital CCD camera and were processed with OpenLab software.

##### Quantitative RT-PCR

Synchronized wild-type, *cep-1(w40)*, *cep-1(gk138)*, *glp-4(bn2)*, and *hus-1(op244)* adult hermaphrodites were irradiated with 100 Gy of X-rays and were left for 3 hr to recover. *glp-4(bn2)* worms were grown at the nonpermissive temperature, and 90–100 worms were selected that lacked a germline. Total RNA was isolated with RNazol B (ams Biotechnology) according to the manufacturer's protocol, treated with DnaseI, and further purified with the RNeasy kit (Qiagen). For cDNA synthesis, purified total RNA was reverse transcribed with 250 U MultiScribe Reverse Transcriptase (Applied Biosystems) by using random primers. Relative amounts of *egl-1* cDNA were subsequently estimated by real-time quantitative PCR in an ABI Prism 7700 Sequence detector system, by using the primers 5'-CAGGACTTCTCCTCGTGAAGATTTC-3' and 5'-GAAAGTCATCG CACATTGCTGCTA-3', which span the single *egl-1* intron. 18S rRNA was used for the internal standard. Average fold induction represents the relative expression of *egl-1* following irradiation (sample)

compared to the untreated control (calibrator), normalized based on 18S rRNA levels.

#### Supplementary Material

Supplementary Material including comparative data of cell cycle arrest and radiation sensitivities of both *hus-1* alleles (Figure S1) as well as additional methodological detail is available at <http://images.cellpress.com/supmat/supmatin.htm>.

#### Acknowledgments

We thank B. Derry and J. Rothman for the *cep-1(w40)* mutant and the *C. elegans* Knockout Consortium for *cep-1(gk138)*; V. Pratis and J. Austin for the *unc-119* genomic rescuing plasmid and the bombardment protocol; A. Fire for pPD117.01, pPD135.83, and pPD129.36; Y. Kohara for cDNA clone yk238e9; A. Coulson for the cTel55x plasmid; and A. Brincat for help with bombardment. We thank A. Hajnal and members of the Hengartner Lab for comments. Some *C. elegans* strains were obtained from the *Caenorhabditis* Genetics Center, which is funded by the National Institutes of Health (NIH) National Center for Research Resources (NCRR). This work was supported by grants from the NIH (GM52540 to M.O.H., F32 GM20801 to E.R.H., and 7 R33 CA81658-02 to S.J.B. and M.V.) and the Ernst Hadorn Foundation (to M.O.H.).

Received: May 12, 2002

Revised: September 18, 2002

Accepted: September 23, 2002

Published: November 19, 2002

#### References

1. Hoeijmakers, J.H. (2001). Genome maintenance mechanisms for preventing cancer. *Nature* 411, 366–374.
2. Rich, T., Allen, R.L., and Wyllie, A.H. (2000). Defying death after DNA damage. *Nature* 407, 777–783.
3. Bach, S.P., Renehan, A.G., and Potten, C.S. (2000). Stem cells: the intestinal stem cell as a paradigm. *Carcinogenesis* 21, 469–476.
4. Heyer, B.S., MacAuley, A., Behrendtsen, O., and Werb, Z. (2000). Hypersensitivity to DNA damage leads to increased apoptosis during early mouse development. *Genes Dev.* 14, 2072–2084.
5. Murakami, H., and Nurse, P. (2000). DNA replication and damage checkpoints and meiotic cell cycle controls in the fission and budding yeasts. *Biochem. J.* 349, 1–12.
6. Bentley, N.J., Holtzman, D.A., Flaggs, G., Keegan, K.S., DeMaggio, A., Ford, J.C., Hoekstra, M., and Carr, A.M. (1996). The *Schizosaccharomyces pombe rad3* checkpoint gene. *EMBO J.* 15, 6641–6651.
7. Horvitz, H.R. (1999). Genetic control of programmed cell death in the nematode *Caenorhabditis elegans*. *Cancer Res.* 59, 1701s–1706s.
8. Gumieny, T.L., Lambie, E., Hartwig, E., Horvitz, H.R., and Hengartner, M.O. (1999). Genetic control of programmed cell death in the *Caenorhabditis elegans* hermaphrodite germline. *Development* 126, 1011–1022.
9. Gartner, A., Milstein, S., Ahmed, S., Hodgkin, J., and Hengartner, M.O. (2000). A conserved checkpoint pathway mediates DNA damage-induced apoptosis and cell cycle arrest in *C. elegans*. *Mol. Cell* 5, 435–443.
10. Hofmann, E.R., Milstein, S., and Hengartner, M.O. (2000). DNA damage-induced checkpoint pathways in the nematode *Caenorhabditis elegans*. *Cold Spring Harb. Symp. Quant. Biol.* 65, 467–473.
11. Ahmed, S., Alpi, A., Hengartner, M.O., and Gartner, A. (2001). *C. elegans* RAD-5/CLK-2 defines a new DNA damage checkpoint protein. *Curr. Biol.* 11, 1934–1944.
12. Derry, W.B., Putzke, A.P., and Rothman, J.H. (2001). *Caenorhabditis elegans* p53: role in apoptosis, meiosis, and stress resistance. *Science* 294, 591–595.
13. Schumacher, B., Hofmann, K., Boulton, S., and Gartner, A. (2001). The *C. elegans* homolog of the p53 tumor suppressor

- is required for DNA damage-induced apoptosis. *Curr. Biol.* **11**, 1722–1727.
14. Venclovas, C., and Thelen, M.P. (2000). Structure-based predictions of Rad1, Rad9, Hus1 and Rad17 participation in sliding clamp and clamp-loading complexes. *Nucleic Acids Res.* **28**, 2481–2493.
  15. Boulton, S.J., Gartner, A., Reboul, J., Vaglio, P., Dyson, N., Hill, D.E., and Vidal, M. (2002). Combined functional genomic maps of the *C. elegans* DNA damage response. *Science* **295**, 127–131.
  16. Caspari, T., Dahlen, M., Kanter-Smoler, G., Lindsay, H.D., Hofmann, K., Papadimitriou, K., Sunnerhagen, P., and Carr, A.M. (2000). Characterization of *Schizosaccharomyces pombe* Hus1: a PCNA-related protein that associates with Rad1 and Rad9. *Mol. Cell. Biol.* **20**, 1254–1262.
  17. Kaur, R., Kostrub, C.F., and Enoch, T. (2001). Structure-function analysis of fission yeast Hus1-Rad1-Rad9 checkpoint complex. *Mol. Biol. Cell* **12**, 3744–3758.
  18. Zou, L., Cortez, D., and Elledge, S.J. (2002). Regulation of ATR substrate selection by Rad17-dependent loading of Rad9 complexes onto chromatin. *Genes Dev.* **16**, 198–208.
  19. Takanami, T., Mori, A., Takahashi, H., and Higashitani, A. (2000). Hyper-resistance of meiotic cells to radiation due to a strong expression of a single recA-like gene in *Caenorhabditis elegans*. *Nucleic Acids Res.* **28**, 4232–4236.
  20. Hodgkin, J., Horvitz, H.R., and Brenner, S. (1979). Nondisjunction mutants of the nematode *Caenorhabditis elegans*. *Genetics* **91**, 67–94.
  21. Chin, G.M., and Villeneuve, A.M. (2001). *C. elegans mre-11* is required for meiotic recombination and DNA repair but is dispensable for the meiotic G(2) DNA damage checkpoint. *Genes Dev.* **15**, 522–534.
  22. Ahmed, S., and Hodgkin, J. (2000). MRT-2 checkpoint protein is required for germline immortality and telomere replication in *C. elegans*. *Nature* **403**, 159–164.
  23. Myung, K., Datta, A., and Kolodner, R.D. (2001). Suppression of spontaneous chromosomal rearrangements by S phase checkpoint functions in *Saccharomyces cerevisiae*. *Cell* **104**, 397–408.
  24. Myung, K., Chen, C., and Kolodner, R.D. (2001). Multiple pathways cooperate in the suppression of genome instability in *Saccharomyces cerevisiae*. *Nature* **411**, 1073–1076.
  25. De Stasio, E., Lephoto, C., Azuma, L., Holst, C., Stanislaus, D., and Uttam, J. (1997). Characterization of revertants of *unc-93(e1500)* in *Caenorhabditis elegans* induced by N-ethyl-N-nitrosourea. *Genetics* **147**, 597–608.
  26. Conradt, B., and Horvitz, H.R. (1999). The TRA-1A sex determination protein of *C. elegans* regulates sexually dimorphic cell deaths by repressing the *egl-1* cell death activator gene. *Cell* **98**, 317–327.
  27. Feng, H., Zhong, W., Punksodsy, G., Gu, S., Zhou, L., Seabolt, E.K., and Kipreos, E.T. (1999). CUL-2 is required for the G1-to-S-phase transition and mitotic chromosome condensation in *Caenorhabditis elegans*. *Nat. Cell Biol.* **1**, 486–492.
  28. Hong, Y., Roy, R., and Ambros, V. (1998). Developmental regulation of a cyclin-dependent kinase inhibitor controls postembryonic cell cycle progression in *Caenorhabditis elegans*. *Development* **125**, 3585–3597.
  29. Bunz, F., Dutriaux, A., Lengauer, C., Waldman, T., Zhou, S., Brown, J.P., Sedivy, J.M., Kinzler, K.W., and Vogelstein, B. (1998). Requirement for p53 and p21 to sustain G2 arrest after DNA damage. *Science* **282**, 1497–1501.
  30. Weiss, R.S., Enoch, T., and Leder, P. (2000). Inactivation of mouse Hus1 results in genomic instability and impaired responses to genotoxic stress. *Genes Dev.* **14**, 1886–1898.
  31. Dahlen, M., Olsson, T., Kanter-Smoler, G., Ramne, A., and Sunnerhagen, P. (1998). Regulation of telomere length by checkpoint genes in *Schizosaccharomyces pombe*. *Mol. Biol. Cell* **9**, 611–621.
  32. Ollmann, M., Young, L.M., Di Como, C.J., Karim, F., Belvin, M., Robertson, S., Whittaker, K., Demsky, M., Fisher, W.W., Buchman, A., et al. (2000). *Drosophila* p53 is a structural and functional homolog of the tumor suppressor p53. *Cell* **101**, 91–101.
  33. Boxem, M., Srinivasan, D.G., and van den Heuvel, S. (1999). The *Caenorhabditis elegans* gene *ncc-1* encodes a *cdc2*-related kinase required for M phase in meiotic and mitotic cell divisions, but not for S phase. *Development* **126**, 2227–2239.
  34. Ashcroft, N., and Golden, A. (2002). CDC-25.1 regulates germline proliferation in *Caenorhabditis elegans*. *Genesis* **33**, 1–7.
  35. Miyashita, T., and Reed, J.C. (1995). Tumor suppressor p53 is a direct transcriptional activator of the human Bax gene. *Cell* **80**, 293–299.
  36. Oda, E., Ohki, R., Murasawa, H., Nemoto, J., Shibue, T., Yamashita, T., Tokino, T., Taniguchi, T., and Tanaka, N. (2000). Noxa, a BH3-only member of the Bcl-2 family and candidate mediator of p53-induced apoptosis. *Science* **288**, 1053–1058.
  37. Nakano, K., and Vousden, K.H. (2001). PUMA, a novel proapoptotic gene, is induced by p53. *Mol. Cell* **7**, 683–694.
  38. Yu, J., Zhang, L., Hwang, P.M., Kinzler, K.W., and Vogelstein, B. (2001). PUMA induces the rapid apoptosis of colorectal cancer cells. *Mol. Cell* **7**, 673–682.
  39. Barlow, C., Brown, K.D., Deng, C.X., Tagle, D.A., and Wynshaw-Boris, A. (1997). Atm selectively regulates distinct p53-dependent cell-cycle checkpoint and apoptotic pathways. *Nat. Genet.* **17**, 453–456.
  40. Weiss, R.S., Matsuoka, S., Elledge, S.J., and Leder, P. (2002). Hus1 acts upstream of Chk1 in a mammalian DNA damage response pathway. *Curr. Biol.* **12**, 73–77.
  41. Herzog, K.H., Chong, M.J., Kapsetaki, M., Morgan, J.I., and McKinnon, P.J. (1998). Requirement for Atm in ionizing radiation-induced cell death in the developing central nervous system. *Science* **280**, 1089–1091.
  42. Symonds, H., Krall, L., Remington, L., Saenz-Robles, M., Lowe, S., Jacks, T., and Van Dyke, T. (1994). p53-dependent apoptosis suppresses tumor growth and progression *in vivo*. *Cell* **78**, 703–711.
  43. Liu, Q., Guntuku, S., Cui, X.S., Matsuoka, S., Cortez, D., Tamai, K., Luo, G., Carattini-Rivera, S., DeMayo, F., Bradley, A., et al. (2000). Chk1 is an essential kinase that is regulated by Atr and required for the G(2)/M DNA damage checkpoint. *Genes Dev.* **14**, 1448–1459.
  44. Brown, E.J., and Baltimore, D. (2000). ATR disruption leads to chromosomal fragmentation and early embryonic lethality. *Genes Dev.* **14**, 397–402.
  45. Jansen, G., Hazendonk, E., Thijssen, K.L., and Plasterk, R.H. (1997). Reverse genetics by chemical mutagenesis in *Caenorhabditis elegans*. *Nat. Genet.* **17**, 119–121.
  46. Praitis, V., Casey, E., Collar, D., and Austin, J. (2001). Creation of low-copy integrated transgenic lines in *Caenorhabditis elegans*. *Genetics* **157**, 1217–1226.
  47. Greenwald, I.S., and Horvitz, H.R. (1980). *unc-93(e1500)*: a behavioral mutant of *Caenorhabditis elegans* that defines a gene with a wild-type null phenotype. *Genetics* **96**, 147–164.